Research Square

Preprints are preliminary reports that have not undergone peer review.
They should not be considered conclusive, used to inform clinical practice,
or referenced by the media as validated information.

Magnetic Resonance Imaging of Müllerian Remnants in Phenotypically Female Patients: A Study of Imaging Features and Interobserver Agreement

Ghada Ali AboElfath Sheta

ghadamed11@yahoo.com

Cairo University

Soha Talaat Hamed

Cairo University

Shereen Mohamed Abdelraouf Khalil

Cairo University

Maha Mohammed Amer

Cairo University

Reham Refaie

Cairo University

Research Article

Keywords: Müllerian remnants, Mayer-Rokitansky-Küster-Hauser syndrome, Gonadal dysgenesis, Unicornuate Uterus, Magnetic Resonance Imaging

Posted Date: November 19th, 2026

DOI: https://doi.org/10.21203/rs.3.rs-11614569/v1

License: This work is licensed under a Creative Commons Attribution 4.0 International License.
Read Full License

Additional Declarations: No competing interests reported.

Magnetic Resonance Imaging of Müllerian Remnants in Phenotypically Female Patients: A Study of Imaging Features and Interobserver Agreement

Abstract

Background: Magnetic resonance imaging (MRI) is the preferred imaging modality for evaluating Müllerian remnants. This study aimed to assess interobserver agreement of MRI features of Müllerian duct remnants (uterine buds, converging fibrous band and triangular cord sign) and the associated ovarian, vaginal and extrauterine findings, using a structured reporting checklist.

Material and Methods: This retrospective single-center study reviewed MRI examinations of consecutive patients referred for suspected or known congenital uterine anomalies between September 2023 and December 2025 (n = 109). Sixty-eight females aged ≥15 years with an absent uterus or a unicornuate uterus were included. MRI was performed on a 1.5 T scanner. Two observers blinded to clinical data, karyotype, and each other's readings, independently reviewed the images using a structured checklist for our study (MOVE: Müllerian remnants, Ovaries, Vagina, Extrauterine anomalies). A senior radiologist resolved disagreements and established the final diagnosis by integrating the MRI findings with clinical data and karyotype (available in 49 patients). Interobserver agreement was assessed using Cohen's κ for categorical variables and Lin's concordance correlation coefficient (CCC) for continuous variables, calculated on the independent readings before adjudication.

Results: Sixty-eight patients (mean age 20 ± 4.9 years) were included, 69.1% presented with primary amenorrhea. Interobserver agreement was moderate for signal characterization on both

sides (κ = 0.54 for right side, 0.55 for left side), substantial for laterality of buds (κ = 0.79), and for fibrous band (κ = 0.88), almost perfect for triangular cord sign (κ = 0.91), vaginal canalization (κ = 0.87) and extrauterine anomalies (κ = 0.96, 95% CI 0.87–1.00). Lin's CCC was excellent for bud volume (CCC=0.969 for right side, 0.968 for left side), triangular cord volume (CCC=0.999), ovarian volume (CCC= 0.997) and vaginal length (CCC= 0.97).

Conclusion: MRI provides reproducible assessment of Müllerian remnants, particularly the triad of Mayer-Rokitansky-Küster-Hauser syndrome (MRKH), with substantial to almost perfect interobserver agreement. A bud that is in close relation to the ipsilateral ovary may mimic a separate gonadal component and in this case, karyotype is needed to settle the radiological diagnosis. A structured checklist can support consistent diagnosis and reporting.

Keywords: Müllerian remnants; Mayer-Rokitansky-Küster-Hauser syndrome; Gonadal dysgenesis; Unicornuate Uterus; Magnetic Resonance Imaging.

1. Introduction:

The disturbance in the development of the paired Müllerian ducts, which normally give rise to the uterus, fallopian tubes, cervix, and upper two thirds of the vagina, results in Müllerian duct anomalies. These anomalies are associated with reproductive problems such as primary amenorrhea, endometriosis, infertility, and obstetric complications such as ectopic pregnancy [1].

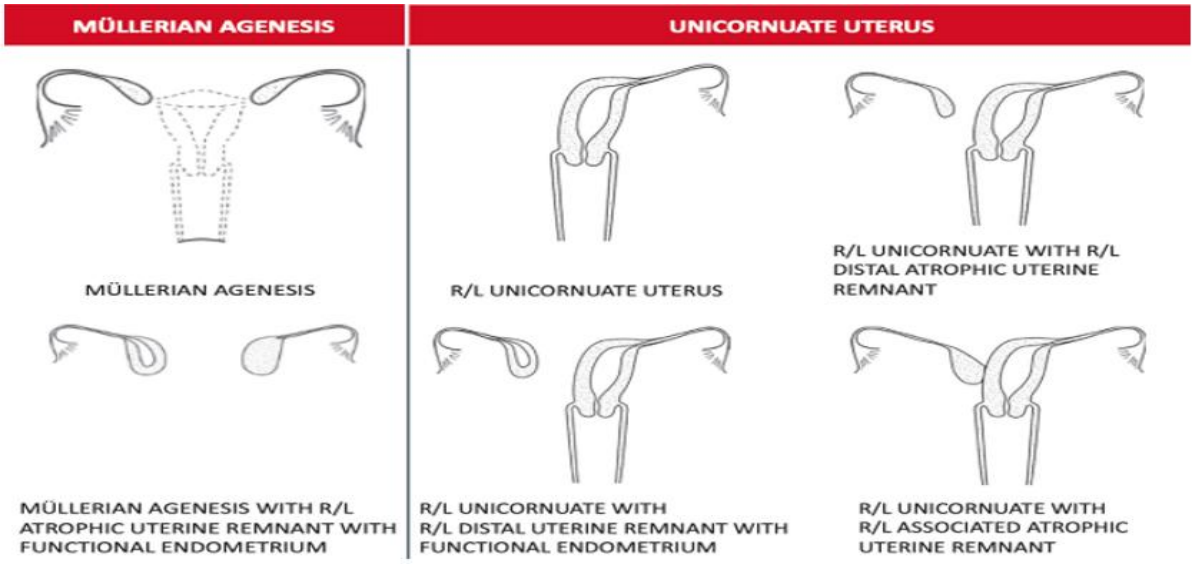
Müllerian development is independent of gonadal development. Conversely, the process is closely related to the development of the urinary tract, and therefore renal anomalies are often diagnosed in patients with Müllerian anomalies [2].

According to the American Society for Reproductive Medicine (ASRM) Müllerian Anomalies Classification 2021, bilateral Müllerian remnants or complete absence of them are categorized as Müllerian agenesis, which may occur with or without associated gonadal dysgenesis. In contrast, a unilateral Müllerian remnant in unicornuate uterus is known as rudimentary horn may be present with variable morphology, cavitation, and degree of communication **(Fig.1)** [3].

Evaluation of a Müllerian remnant poses diagnostic challenges, as the rudimentary structure often comprises predominantly fibrous tissue or smooth musculature without endometrium, yielding diffuse intermediate T2 signal. Such signal may render it radiologically indistinguishable from abnormal gonads or adjacent adnexal structures, especially when spatially proximate [4].

Fig.1: ASRM 2021 categories of Müllerian remnants. Unlike the American Fertility Society (AFS) classification, anomaly categories are no longer numbered but instead are identified by descriptive terminology [3].

Mayer-Rokitansky-Küster-Hauser syndrome (MRKH) was described by Mayer in 1829 and



Rokitansky in 1838 while Hauser in 1961 described the distinguishing features of MRKH from androgen insensitivity syndrome. Most patients with MRKH have unilateral or bilateral

rudimentary uteri, with varying sizes and degrees of differentiation of the zonal anatomy, and they are found to maintain a caudal relationship to the ovaries [5,6].

As secondary sexual characters are normally developed in MRKH patients, they usually go undetected until adolescence presenting with primary amenorrhea. It is categorized into two types, type I (typical) and type II (atypical) based on absence or presence of associated anomalies respectively [2]. Urological abnormalities associated with Type II MRKH are renal ectopia, horseshoe kidney and rarely renal agenesis. Varying degrees of musculoskeletal anomalies have been noted [5].

Pelvic ultrasonography (US) is the initial modality of assessment; however, MRI is more sensitive in the evaluation of the gonads. When the gonads are not visualized in imaging, laparoscopic pelvic examination or even biopsy of intra-abdominal gonads may be required in the management of intersex disorders [7].

MRI features of Müllerian remnants in MRKH consist of three structural components: bilateral uterine buds, fibrous band-like structures, and midline triangular soft tissue. These features play a pivotal role in distinguishing MRKH from complete androgen insensitivity syndrome (CAIS) and other differential diagnoses [8,9].

On MRI, the non-functioning rudimentary horn in cases of unicornuate uterus is usually asymptomatic and discovered incidentally, and it appears as a small, solid soft-tissue structure lacking an endometrial cavity or zonal anatomy. Unlike a functioning cavitary horn, which may show hematometra and cyclic changes [4].

In this study, the term “Müllerian developmental failure” is used as a descriptive embryological umbrella term to encompass Müllerian agenesis presenting as either bilateral uterine agenesis or unilateral uterine development, including a unicornuate uterus with or without a rudimentary horn. This terminology is adopted for the purpose of the present study and does not represent a separate diagnostic classification.

Our study aimed to describe the spectrum of MRI features of Müllerian remnants in phenotypic females with Müllerian developmental failure, either bilateral or unilateral, following a structured reporting checklist, **MOVE**: Müllerian remnants (bud, band, cord sign), Ovaries, Vagina, and Extrauterine anomalies, and to assess the interobserver agreement of the checklist items.

2. Materials and Methods:

This retrospective study was approved by the research ethics committee (REC) of our institution, in accordance with the declaration of Helsinki. The involved data were collected from the Picture Archiving and Communication System (PACS) archive of the Radiology department of our institution. All patients who were referred from the Department of Gynecology and Obstetrics for diagnosis or confirmation of suspected or known congenital uterine anomalies between September 2023 and December 2025 were consecutively identified, irrespective of the final diagnosis (n = 109). After applying the exclusion criteria, a junior radiologist not involved in image interpretation, selected 68 eligible patients **(Fig. 2).**

The inclusion criteria comprised phenotypically females aged ≥ 15 years whose MRI demonstrated absent **or** unicornuate uterus. Patients with other anomalies that showed uterus were excluded, such as uterus didelphys, bicornuate, septate uterus and obstructive anomalies in the form of imperforate hymen or transverse vaginal septum. Two cases diagnosed as CAIS were

excluded as both testicles were noted within the inguinal canal and the patients were younger than 5 years old.

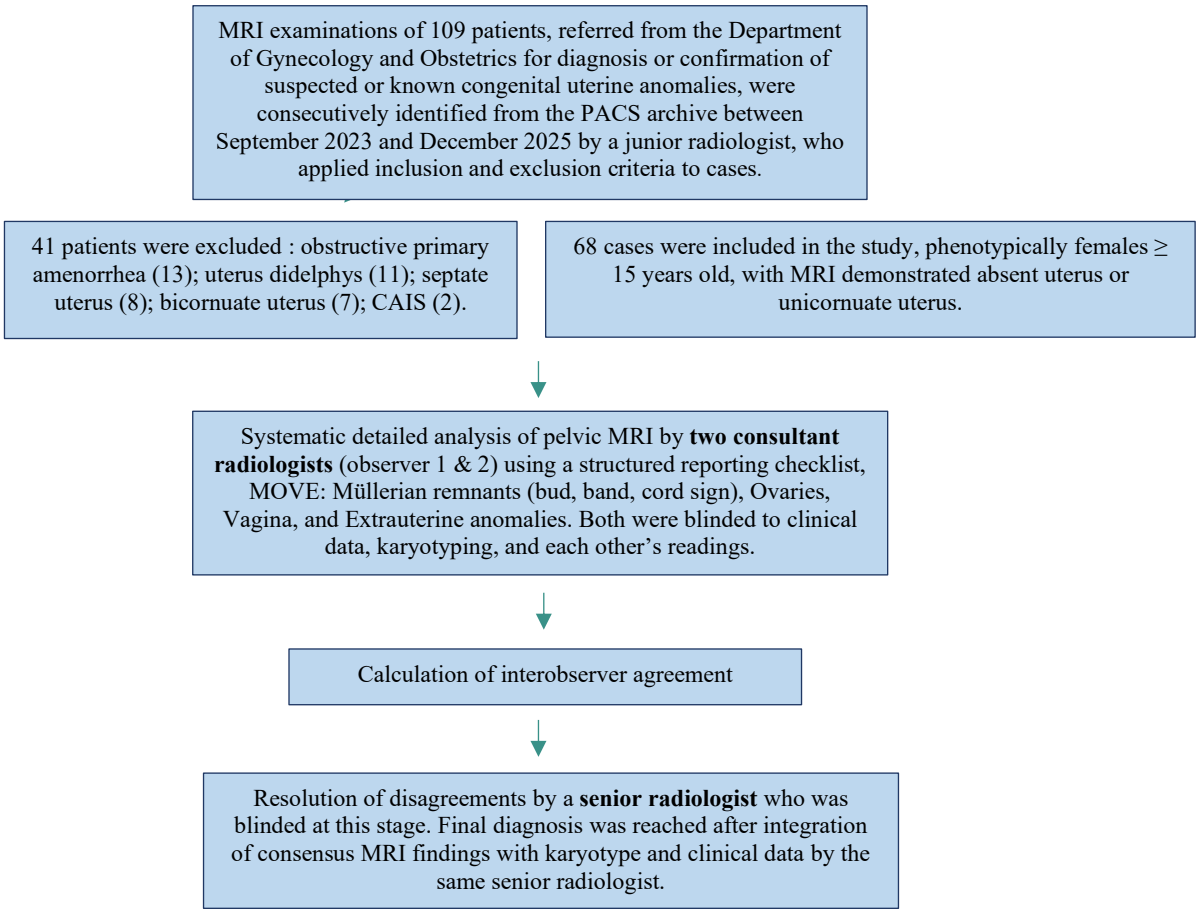


Fig. 2 : Flowchart of patient selection and study workflow.

Technique of MRI:

The MRI examinations were performed using 1.5 T MRI scanner (Achieva Philips 32 channels, Netherlands), pelvic coil. Patients were positioned supine. After a localizer scan, T2-weighted images (T2WI) axial, coronal, and sagittal fast spin echo sequences were obtained (TR/TE 3230-4080/93 msec, Field of view (FOV): 22 x 22 cm; Slice thickness: 5 mm, matrix 512 x 307).T1-weighted images (T1WI) axial fast spin-echo sequence (TR/TE, 762/14 msec; FOV: 22 x 22 cm,

matrix, 512 x 307) , were obtained from the aortic bifurcation to the symphysis pubis. T2 sagittal was obtained with zero angle to the vagina. T2WI coronal of the abdomen was also requested to detect co-existence of renal anomalies . Axial diffusion weighted image (DWI) with different b values (b 0, 800) as well as apparent diffusion co-efficient (ADC) mapping which was automatically reconstructed on a post-processing workstation, FOV: 45 cm, Slice thickness: 5 mm, 256×256 matrix. Diffusion restriction was qualitatively defined as hyperintensity on DWI accompanied by corresponding hypointensity on the ADC map. No quantitative region-of-interest (ROI) measurements of ADC values were performed due to the small, non-target or rudimentary nature of the uterine buds, which renders focal quantitative measurements susceptible to volume averaging artifacts.

Image analysis and interpretation of MRI findings:

MRI examinations were independently reviewed by two consultant radiologists (~10 years of experience in pelvic imaging) who were blinded to clinical data, karyotyping results (when available) and to each other's readings. Both observers followed a structured reporting checklist, **MOVE**: **M**üllerian remnants, **O**varies, **V**agina, and **E**xtrauterine anomalies. In cases of disagreement, the final interpretation was determined by a senior radiologist (~20 years of experience in women imaging) from the study team, who was also blinded to the karyotype, hormonal profile, and clinical data at that stage. Subsequently, the same radiologist reviewed the available karyotype results and clinical data and integrated them with the consensus MRI findings to establish the final diagnosis of each case.

Before the formal reading, both observers were trained on a separate set of 20 MRI examinations of Müllerian anomalies, during which the checklist items and their definitions were reviewed. These 20 cases were not included in the study cohort.

- **[M] Müllerian remnants:** Müllerian developmental failure (either bilateral or unilateral) is replaced by variable degrees of uterine remnant development, ranging from complete absence of Müllerian tissue to rudimentary structures. The typical cases of bilateral Müllerian developmental failure showed the triad of: 1) Uterine buds: pelvic oblong-shaped soft tissue structures of intermediate signal intensity in all pulse sequences with no restriction in DWIs. 2) Low signal fibrous band-like structure connecting both uterine buds together or connecting the rudimentary horn to the unicornuate uterus. 3) Both buds converge at the midline triangular soft tissue lying over the bladder dome (triangular cord sign).

In each case, uterine buds were evaluated for: Presence (unilateral or bilateral) or complete absence of buds. Signal intensity (T1, T2, DWI), presence or absence of masses, volume which was calculated using the prolate ellipsoid formula (0.52 x length x width x height).

- **[O] Ovaries:** were analyzed for their: existence or absence (streak) and size: considered average if (3-10 cm^3), small if (< 3 cm^3), enlarged if (> 10 cm^3). The location and relation to the uterine buds: cranial or caudal, adherent or separable but connected to bud by a thin low-signal fibrous band. When the uterine bud was absent, the ovarian location was considered normal if seen within the ovarian fossa, high pelvic if located higher than normal but still intrapelvic, herniated if within the inguinal canal, or ectopic if located in the iliac fossa.
- **[V] Vagina:** was evaluated for length and degree of canalization on sagittal and axial T2WI MRI sequences, with assessment of its two embryologically distinct segments (the upper two-

thirds and the lower one-third). The vagina is considered non canalized if the normal H-shaped lumen in not visualized or collapsed low-to-intermediate T2 signal intensity vaginal canal. In this case the observers measured the length of the solid fibromuscular band or fibrous tissue sheet.

- **[E] Extrauterine anomalies:** The presence of associated renal, external genitalia or lumbosacral vertebral anomalies were evaluated in detail.

***Reference standard:** Pathological confirmation of Müllerian remnant identity was not performed in this cohort, except in one case of mixed gonadal dysgenesis (MGD), as surgical exploration is not clinically indicated in the majority of those patients and would expose them to unnecessary operative risk in the absence of a therapeutic indication. Karyotyping was available for 49 cases (47 cases of Müllerian agenesis and 2 cases of unicornuate uterus).

The final diagnosis was established by integrating the available imaging findings supported by the reference reading of senior radiologist, clinical data and karyotyping results when available. The diagnoses were MRKH syndrome, gonadal dysgenesis with Müllerian agenesis, and unicornuate uterus with or without rudimentary horn. These conditions were grouped because they share failure of Müllerian duct development, which is bilateral in MRKH and in gonadal dysgenesis with Müllerian agenesis, and unilateral in unicornuate uterus.

***Statistical analysis:** Data were collected and organized using Microsoft Excel. Statistical analyses were performed using Jamovi statistical software, version 2.7.12. Qualitative variables were summarized as frequencies and percentages.Age was summarized as mean ± standard deviation (SD), whereas quantitative variables were expressed as median with interquartile range (IQR). Interobserver agreement was calculated for MRI items in the checklist using Cohen's κ

coefficient with its standard error and 95% confidence interval [10]. κ values were interpreted according to Landis and Koch as follows: <0.20 slight, 0.21-0.40 fair, 0.41-0.60 moderate, 0.61-0.80 substantial, and >0.80 almost perfect agreement [11]. For continuous variables (uterine bud volume, ovarian volume and vaginal length), agreement was assessed using Lin's concordance correlation coefficient (CCC) with its 95% confidence interval (CI) [12]. The analysis was performed using paired measurements of the same anatomical structures obtained independently by both observers. The number of paired measurements included in each analysis was reported accordingly. Both values were calculated on the two observers' independent readings, before the senior radiologist resolved disagreements.

3. Results:

The study included 68 patients with a mean age of 20 ± 4.9 years. The most common presentation was primary amenorrhea (47/68, 69.1%), followed by unilateral cyclic abdominal pain (9, 13.2%), primary infertility (6, 8.8%), oligomenorrhea (5, 7.4%), and a positive pregnancy test (1, 1.5%). Karyotype results were available for 49 patients, the final diagnosis was established after review of their reports **(Table 1)**.

Table 1: Karyotyping distribution relative to the final diagnosis conducted by the senior radiologist (n = 68)

Diagnosis	n (%)	Karyotyped, n	46, XX, n	Abnormal karyotype, n (type)
MRKH syndrome	**35 (51.5)**	**35**	**35**	**0**
– MRKH type I	26 (38.2)			
– MRKH type II	9 (13.2)			

Gonadal dysgenesis with – Müllerian agenesis – Mixed gonadal dysgenesis (MGD)	**12 (17.6)** 11 (16.2) 1 (1.5)	**12**	**6**	**6** 45, X (4)[a]; 46, X + marker chromosome (1)[b] 45, X/46, XY mosaicism (1)[c]
Unicornuate uterus – Non-functioning rudimentary horn – Functioning non-communicating horn – No rudimentary horn, normal ovaries – No rudimentary horn, gonadal dysgenesis – Gestational sac in rudimentary horn	**21 (30.9)** 9 (13.2) 7 (10.3) 2 (2.95) 2 (2.95) 1(1.5)	**2**	**1**	45, X (1)[a]
Total	**68 (100)**	**49**	**42**	**7**

[a] *Turner syndrome,* [b] *Turner with marker chromosome,* [c] *Sex chromosome mosaicism*

3.1. Müllerian remnants involved 3 items:

A. Uterine buds

Evaluation of the presence and laterality of uterine buds in the 68 patients in relation to the final diagnosis was demonstrated in **Table 2.**

Table 2 : Presence and laterality of uterine buds in relation to the final diagnosis (n = 68)

Uterine buds	Observer 1, n	Observer 2, n	Senior, n (%)	Final diagnosis (n)	κ (95% CI)
Present (total)	**42**	**35**	**43 (63.2)**		**0.79 (0.67 to 0.91)**
Unilateral	21	22	22 (32.4)	MRKH (4); rudimentary horn in unicornuate uterus (17); MGD (1)	
Bilateral	21	13	21 (30.9)	MRKH (21)	
Absent (total)	**26**	**33**	**25 (36.8)**		
Bilateral absence	22	29	21 (30.9)	MRKH (10); gonadal dysgenesis (11)	
Unilateral absence	4	4	4 (5.9)	Unicornuate uterus without contralateral rudimentary horn (4)	

Interobserver agreement was substantial (κ = 0.79; 95% CI 0.67-0.91). Observer 2 identified fewer buds than observer 1 (35 vs 42 patients), mainly because five cases with bilateral buds were interpreted by observer 2 as ovotestes. Unilateral bud absence in 4 patients was detected in

unicornuate uterus, whereas bilateral absence occurred in 10 patients reported by the senior radiologist as MRKH syndrome and 11 patients as gonadal dysgenesis.

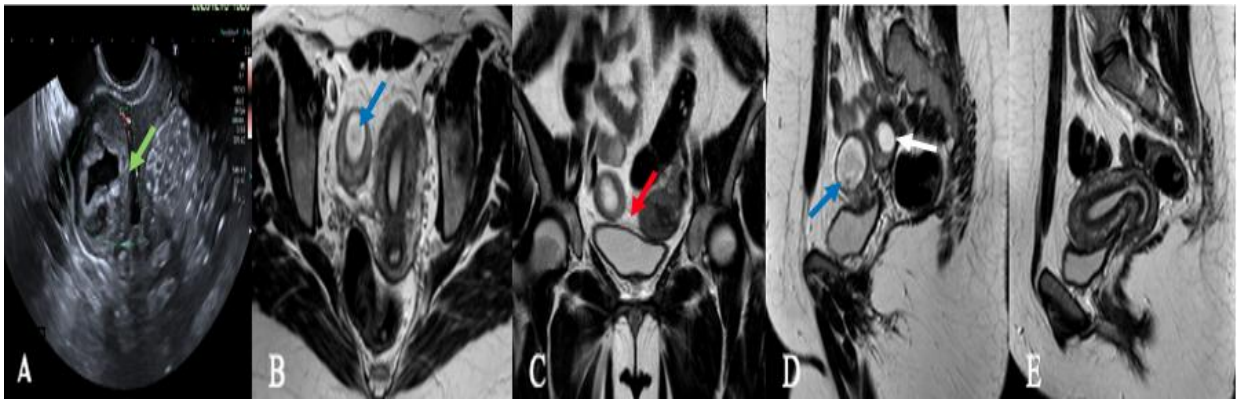


Table 3: MRI features of uterine buds on each side

Parameter	Observer 1, n	Observer 2, n	Senior, n (%)	κ (95% CI)/ Lin's CCC
Right uterine buds, n/68 (%)	**30**	**23**	**31 (45.6)**	
▪ Oblong shape, intermediate T2 signal, no diffusion restriction	22	15	23 (74.2)	
▪ Intracavitary blood products	4	4	4 (12.9)	**0.54 (0.27 to 0.81)**
▪ Thin endometrium (≈3 mm)	2	2	2 (6.5)	
▪ Diffuse low signal intensity	1	1	1 (3.2)	
▪ Rudimentary horn with cystic component	1	1	1 (3.2)	
Volume (cm^3), median (IQR) (n of paired measurement =**23**)	1.57 (1.05 to 4.97) cm^3	1.36 (0.26 to 4.10) cm^3		**0.969 (0.937 to 0.985)**
Left uterine buds, n/68 (%)	**33**	**25**	**33 (48.5)**	
▪ Oblong shape, intermediate T2 signal, no diffusion restriction	25	16	25 (75.8)	
▪ Intracavitary blood products	4	4	4 (12.1)	**0.55 (0.29 to 0.80)**
▪ Thin endometrium	4	4	4 (12.1)	
Volume (cm^3), median (IQR) (n of paired measurement =**25)**	1.58 (0.76 to 3.71) cm^3	1.4 (0.52 to 3.6) cm^3		**0.968 (0.936 to 0.984)**

As demonstrated in **Table 3**, most uterine buds exhibited an oblong morphology with intermediate T2 signal intensity and no diffusion restriction. Both observers reported one rudimentary horn as distended by fluid signal. This case was reported as a rudimentary horn harbored a gestational sac as a final diagnosis by the senior radiologist as the patient had positive pregnancy test **(Fig.3).**

Fig. 3: Gestational sac in rudimentary horn. 28 years old lady with +ve pregnancy test. **A)** Transvaginal ultrasound (TVUS) revealed right adnexal disrupted gestational sac separable from the ipsilateral ovary (green arrow). **B)** axial T2WI revealed left unicornuate uterus and **M:** both observers reported a right adnexal structure of soft tissue intensity similar to myometrium with eccentric rounded lesion of fluid signal (blue arrow) suggested to be a non-communicating rudimentary horn. **C)** coronal T2WI showed a thin fibrous band connecting the rudimentary horn to the left unicornuate uterus (red arrow). **D, E)** sagittal T2Wis demonstrate the right horn with GS in close proximity to the right **O**vary (white arrow) yet being separable from it. The left horn appeared normal. **V:** canalized average- length left hemivagina. No **E**xtrauterine anomalies.

Observers 1 and 2 disagreed on uterine buds in 10 of 68 patients. In eight patients with bilateral buds according to observer 1, observer 2 recorded no buds: in five, the structures were interpreted as ovotestes (a second gonadal component related to the ipsilateral ovary), and in three they were judged absent. In one patient, observer 1 recorded no buds whereas observer 2 recorded bilateral buds. In another patient, one left-sided structure with homogeneous signal and restricted diffusion was interpreted by observer 2 and the senior radiologist as a probable gonadal structure and was therefore not counted as a uterine bud by either observer. As a result, observer 1 counted more buds than observer 2: 30 vs 23 on the right (8 missed, 1 gained) and 33 vs 25 on the left (8 missed, 1 gained, 1 reclassified as gonadal), a net difference of 7 and 8 respectively.

B. Converging fibrous band:

A fibrous band connecting the uterine buds, or a bud and the contralateral uterine structure, was identified in 34/68 patients (50%) by observer 1, 32/68 (47.1%) by observer 2, and 35/68 (51.5%) by the senior radiologist. Interobserver agreement was almost perfect ($\kappa = 0.88$, 95% CI 0.77–0.99). All four discordant cases were MRKH patients, and the senior radiologist classified all of them as band present (one missed by observer 1 and three by observer 2). In the case with a left-sided abnormal gonadal structure and a right uterine bud, both observers reported an

interconnecting fibrous band. Then observer 2's band counts are consistent with observer 1, and the five ovotestes cases don't affect the fibrous band agreement. In the five cases in which observer 2 interpreted the structure as an ovotestis, the fibrous band was identified by both observers.

C. Triangular cord sign:

A triangular cord sign was identified in 28/68 patients (41.2%) by observer 1, 25/68 (36.8%) by observer 2, and 27/68 (39.7%) by the senior radiologist. Interobserver agreement was almost perfect (κ = 0.91, 95% CI 0.81–1.00). Regarding the presence of cord sign in relation to the final diagnosis, it was seen only in patients with MRKH and gonadal dysgenesis, and in none of the 21 patients with unicornuate uterus. In MRKH it was identified in 24/35 patients (68.6%) by observer 1 and the senior radiologist and in 22/35 (62.9%) by observer 2 (κ = 0.87, 95% CI 0.70–1.00). In gonadal dysgenesis it was identified in 4/12 patients (33.3%) by observer 1 and in 3/12 (25%) by observer 2 and the senior radiologist (κ = 0.80, 95% CI 0.43–1.00). The three discordant cases (two in MRKH and one in gonadal dysgenesis) were all positive for observer 1 and negative for observer 2.

The median cord volume was 1.08 cm^3 (IQR 0.70–1.36) for observer 1, 1.00 cm^3 (0.55–1.27) for observer 2, and 1.06 cm^3 (0.67–1.36) for the senior radiologist, with excellent agreement between the two observers (Lin's CCC = 0.999, 95% CI 0.999–1.000; n of paired measurement = 25).

According to the senior's radiologist, the complete triad was identified in 17/35 (48.6%) patients with MRKH syndrome (25 % of the whole cohort) and in none of the other diagnostic groups.

3.2. Ovaries

In five cases, observer 2 reported ovotestes, with a clearly demarcated second gonadal component related to the lower pole of the ipsilateral ovary. Observer 1 reported the same structures as ovaries with closely related uterine buds. The senior radiologist interpreted them as uterine buds in close proximity to the ovaries, and the diagnosis of MRKH syndrome was supported by the clinical findings and a 46, XX karyotype.

For these five cases, observer 2 measured the volume of the ovary alone and of the whole ovotestis. Only the ovarian volume was used in the agreement analysis, so that both observers' measurements referred to the same structure. The volume of the second component suspected to be abnormal gonads reported by observer 2 ranged from 1.4 to 3 cm^3.

Interobserver agreement for ovarian volume was almost perfect overall (Lin's CCC 0.997; 95% CI 0.996-0.998). In the right side, both observers reported the presence of ovaries in 54 patients with the median volume was 3.52 cm^3 (IQR 2.45-4.69) for observer 1 and 3.50 cm^3 (IQR 2.45-4.76) for observer 2, and Lin's CCC = 0.999 (95% CI 0.9998 to 0.9999; n of paired measurement = 54). In the left side, 55 ovaries were detected with the median volume was 4.61 cm^3 (IQR 3.14-7.26) for observer 1 and 4.61 cm^3 (IQR 3.06-7.96) for observer 2, and Lin's CCC= 0.988 (95% CI 0.981 to 0.992; n of paired measurements 55). In patients with gonadal dysgenesis, no ovaries were detected by either reader.

Among the 54 right-sided and 55 left-sided detected ovaries, an ovary in close proximity to the ipsilateral uterine bud was noted on the right side in 17/30 buds (56.7%) by observer 1 and in 11/23 (47.8%) by observer 2. On the left side, it was noted in 17/33 buds (51.5%) by observer 1 and in 10/25 (40.0%) by observer 2. Overall, close proximity was reported in 34/63 buds (54.0%) by observer 1 and 21/48 (43.8%) by observer 2.

Ovarian location was assessed in 109 ovaries (54 right, 55 left). Both observers agreed on 99 of 109 detected ovaries (90.8%). Among the 49 concordant right-sided ovaries, the ovary was cranial to the bud in 24, caudal in 1, in the ovarian fossa in 15, in a high pelvic position in 8, and herniated in 1. Among the 50 concordant left-sided ovaries, it was cranial to the bud in 19, caudal in 6, in the ovarian fossa in 13, in a high pelvic position in 10, and herniated in 2 **(Fig. 4).** In the remaining 10 ovaries (5 per side), observer 1 reported the ovary as cranial to the bud, whereas observer 2 interpreted the bud-like structure as the second gonadal component of an ovotestis, related to the lower pole of the ipsilateral ovary, so no bud-relative location could be assigned.



Ovarian status was independent of the uterine buds in MRKH and unicornuate uterus, whereas in gonadal dysgenesis the absence of buds paralleled the absence of ovaries **(Table 4)**.

Fig.4: Unilateral uterine bud and left ovary herniation in the inguinal canal in case of MRKH type 1. A 17-year-old girl complained of 1ry amenorrhea, during clinical examination the gynecologist noticed a painful left inguinal mass lesion. **A)** Coronal T2WI image demonstrated **M:** unilateral right uterine bud (blue arrow) of intermediate signal being cranial to the **O:** ipsilateral ovary. **B)** sagittal T2WI image revealed the absence of the midline triangular cord sign and canalization of the lower ~2 cm of the **V**agina. **C, D)** Axial T2WI images revealed the left inguinal painful mass to be a herniated left ovary yet showing preserved follicular activity (white arrow). The right ovary is intrapelvic anteriorly displaced with a hemorrhagic cyst (green arrow). No **E**xtrauterine anomalies. Karyotyping reported 46 XX.

Table 4: Relation between the presence of uterine buds and ovarian status, by final diagnosis (senior radiologist)

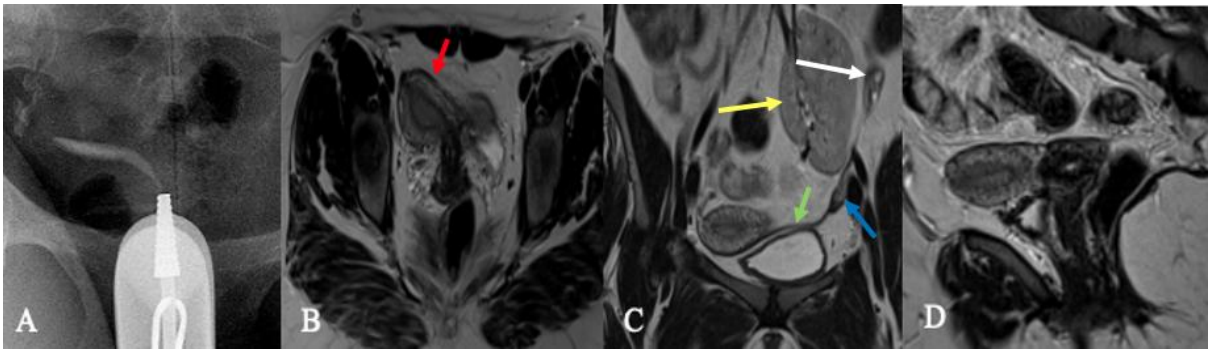
Diagnosis	Uterine buds	Ovarian status	Key observation
MRKH (n = 35)	Present (uni- or bilateral): 25/35	Both ovaries normal: 24/25	Müllerian remnant parallels normal ovarian development
		Unilateral ovarian absence: 1/25 (unilateral bud with ipsilateral ovary; bud and ovary absent on the contralateral side)	Rare associated unilateral gonadal defect
	Absent bilaterally: 10/35	Both ovaries normal 10/10	Müllerian remnant presence is independent of normal ovarian development
Gonadal dysgenesis (n = 12)	Present, unilateral: 1/12	Absent ovary bilateral	Exceptional discordant differentiation (bud in MGD)
	Absent bilaterally: 11/12		Bud absence parallels gonadal absence
Unicornuate uterus (n = 21)	Rudimentary horn present: 17/21	Normal ovaries 17/21	Müllerian remnant parallels normal ovarian development
	No rudimentary horn: 4/21	Normal ovaries in 2/4	Müllerian remnant presence is independent of normal ovarian development
		Absent ovaries bilateral 2/4	Rare combined bilateral gonadal defect

3.3. Vagina

Regarding the vaginal measurement, either canalized or fibrous vaginal remnant, the median length (IQR) was 5.3 cm (2.0–6.4) for observer 1 and 5.0 cm (2.0–6.0) for observer 2. Agreement was excellent across the whole cohort (Lin's CCC = 0.97, 95% CI 0.95–0.98), with a mean difference of 0.13 cm (95% CI −0.02 to 0.28) and 95% limits of agreement from −1.08 to 1.33 cm.

Observer 1 reported non-canalization of the vaginal lumen in 24/68 patients (35.3%), while observer 2 reported 20/68 (29.4%). Thus, the observers agreed in 64/68 patients regrading vaginal canalization (94.1%; $\kappa = 0.87$, 95% CI 0.74–0.99). All four discordant cases were patients with MRKH in whom observer 1 recorded no canalization whereas observer 2 recorded canalization limited to the lower 2 cm of the vagina.

3.4. Extrauterine anomalies

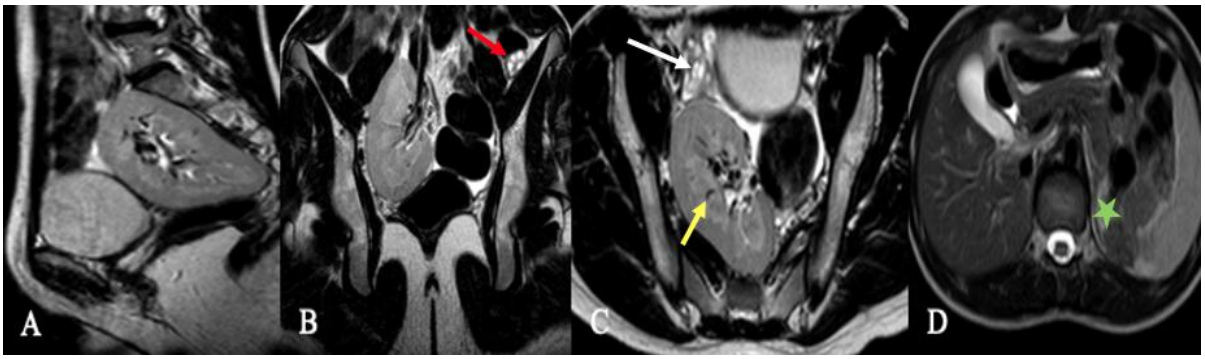


Extrauterine anomalies were detected in 15/68 patients (22.1%) by observer 2 and the senior radiologist and in 14/68 (20.6%) by observer 1. Observer 1 missed one anomaly (a Tarlov cyst), and the two observers were concordant in the remaining 67 of 68 patients (98.5%), corresponding to almost perfect agreement ($\kappa = 0.96$, 95% CI 0.87–1.00).

Unilateral pelvic kidney was identified in 5 cases (7.4%) **(Fig. 5),** while unilateral renal agenesis was observed in 2 cases (2.9%). Bilateral renal anomalies were detected in 3 cases (4.4%) in the form of 2 cases of pelvic kidney with absent other side **(Fig. 6)** and one case of bilateral pelvic kidneys. Unilateral duplex kidney was noted in 1 case (1.5%). Only 4 cases (5.9%) were found to have other anomalies, two of them showed ambiguous genitalia (one with hypertrophied clitoris and the other had a rudimentary penile structure), one with Hirschsprung disease (was reported as a suspected diagnosis manifested by significantly dilated large bowel and abrupt transition at the rectosigmoid with collapsed rectum) and one had Tarlov cyst.

Fig. 5: Ectopic kidney in unicornuate uterus with rudimentary horn. 22 years old lady complained of 1ry infertility for 3 years. **A)** Hysterosalpingography (HSG) revealed a single fusiform cavity off midline inclined to the right side. **B)** axial T2WI showed a well-developed right unicornuate uterus (red arrow)**. C)** coronal T2WI revealed **M**: a small oval shaped structure of homogenous intermediate signal (blue arrow) seen within the left iliac fossa connected to the right horn by a low signal thin fibrous band (green arrow) with similar one extending from it to the left **O**vary (white arrow), representing the left rudimentary uterine bud. **E**xtrauterine anomalies: Ectopic pelvic left kidney is also seen (yellow arrow). Normal right ovary with preserved follicular activity (not shown here). **D)** sagittal T2WI showed the hemicervix and the canalized right hemi**V**agina of developed horn.

Fig. 6: MRKH type 2. 15 years old girl complained of 1ry amenorrhea. **A)** sagittal T2WI image demonstrate **M**: the absence of the midline triangular cord sign, and. **B)** coronal T2WI image shows abnormal high up location of average sized left **O**vary (red arrow) with no evidence of uterine buds or abnormal gonadal tissues. **C)** axial T2WI image show band like non canalized **V**aginal remnant and an **E**xtrauterine anomaly: ectopic pelvic hypertrophied right kidney (yellow arrow) with anteriorly displaced normal right ovary (white arrow) **. D)**Axial T2 abdominal image also revealed absence of the left kidney (star). Karyotyping reported 46 XX.



4. Discussion:

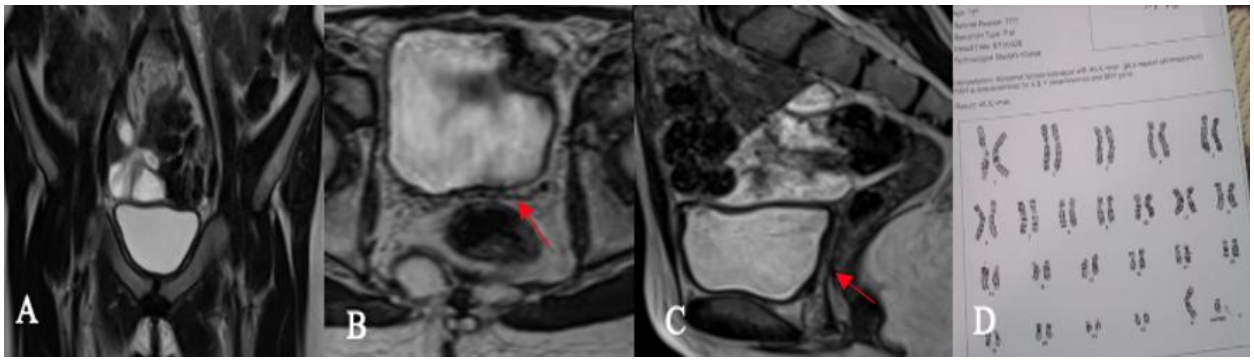
Müllerian remnants in females typically demonstrate signal characteristics analogous to myometrium on MRI, with absent or variably developed zonal anatomy. A defining radiological feature is the absence of a normally formed cervical component, which serves as a key criterion in confirming the diagnosis and differentiating these remnants from other pelvic soft-tissue structures [13,14].

Bilateral Müllerian agenesis has an estimated incidence of approximately 1 in 4,500–5,000 female births and accounts for about 10–15% of congenital Müllerian anomalies. In contrast, unilateral Müllerian agenesis has a higher population prevalence of roughly 1 in 1,000 women and represents approximately 5–10% of Müllerian anomalies [15].

Although these conditions share a Müllerian developmental failure, they are biologically heterogeneous, and some signs (such as the triangular cord sign) are expected to be confined to specific groups. We therefore report agreement for the whole cohort and, where relevant, for MRKH alone.

In our cohort, MRKH type 1 was the most common diagnosis. It represented 74.3% (26/35) of all MRKH syndrome cases. In a large analysis of 1,055 Chinese patients with MRKH syndrome, approximately 69.6% were type I and 30.4% were type 2. Another large European-centered review found that type 1 comprised about 56–72% of cases and type 2 about 28–44%, indicating variation by population and study methodology [16,17].These data confirm that the isolated form is more common overall, but the relative frequency of syndromic presentations varies across cohorts.

Interobserver agreement for the presence and laterality of uterine buds was substantial (κ = 0.79). According to the senior radiologist, uterine buds were present in 63.2% of the cohort, and bilateral buds were seen only in patients with MRKH syndrome (21/35, 60 %), while unilateral buds were found in 4/35 (11.4%) of MRKH patients. These findings are broadly consistent with previous reports. Jaiswal et al. [2] found bilateral buds in 9 of 10 MRKH patients and a solitary bud in one, and a larger MRKH cohort reported bilateral rudimentary remnants in 68.4% and unilateral remnants in 9.7% [18]. Our results are in line with Bhayana et al. [14] who reported that

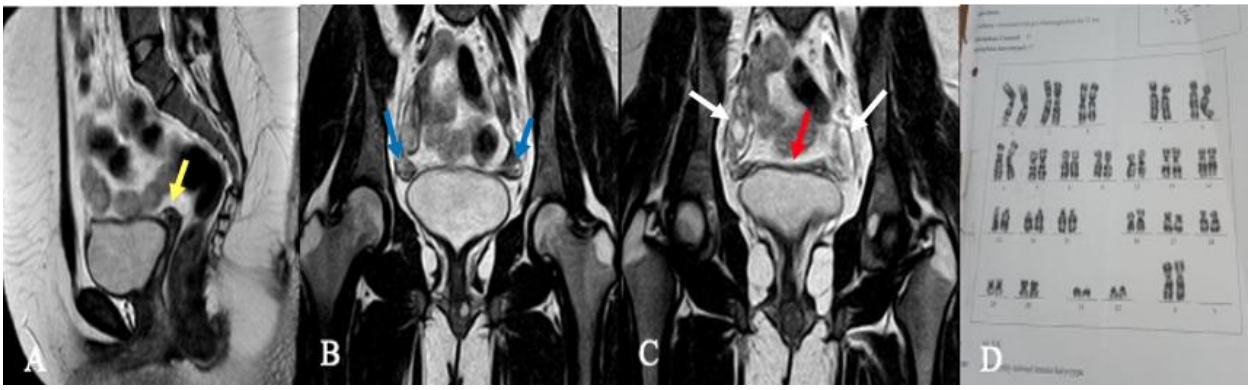


interobserver agreement in assessment of uterine buds in MRKH patients was good to excellent (κ: 0.7788 ± 0.2168 to 1 ± 0).

In our study, complete bilateral absence of uterine buds was found in 11 of 12 patients with gonadal dysgenesis. Six of these had a 46,XX karyotype, four had 45,X , and one had 46,X with marker chromosome **(Fig. 7).** The occurrence of gonadal dysgenesis with a 46,XX karyotype is recognized. Jha et al. [19] described a 24-year-old with 46,XX gonadal dysgenesis complained of primary amenorrhea, poor breast development and unable to conceive since last 6 months, and MRI revealed absent uterus and ovaries, while the vagina was canalized and of average length. Similar cases have been reported by others.

Fig. 7: **Disorders of sex development (DSD).**16 years old girl referred for investigation of 1ry amenorrhea. **A)** coronal T2WI demonstrated **M:** absent uterus and uterine buds with **O**: no identifiable gonadal tissues (no ovaries or testicles). **B, C)** axial and sagittal T2WIs confirm the absence of midline triangular cord sign with **V:** band -like non canalized vagina (red arrows). **D)** karyotyping reported abnormal karyotype (46 X+ marker chromosome). No **E**xtrauterine anomalies.

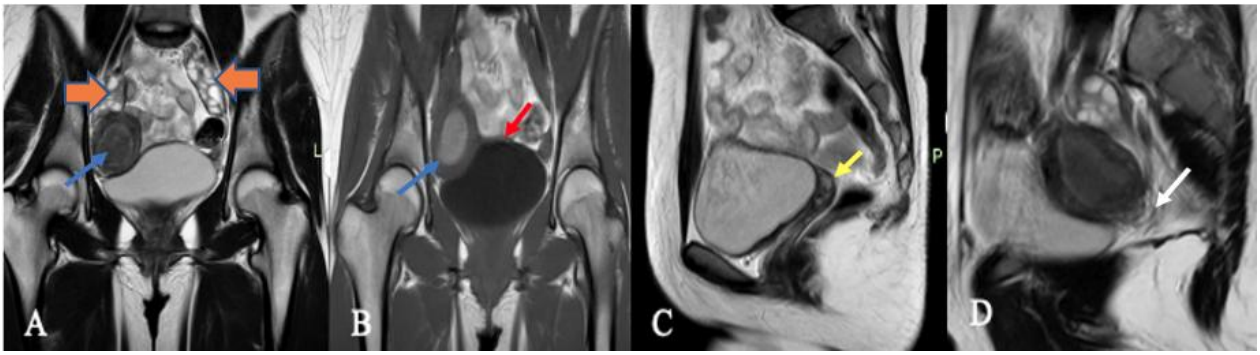
In our study, there was moderate interobserver agreement regarding the uterine buds' morphology and signal intensity (κ = 0.54 for right side, 0.55 for left side). They predominantly exhibited an oblong morphology with intermediate T2 signal intensity and no diffusion restriction. The main diagnostic pitfall was distinguishing a uterine bud adjacent to the ovary from a second



gonadal component, as occurred in five cases that observer 2 interpreted as ovotestes **(Fig. 8).** A bud that is adherent to or closely opposed to the ipsilateral ovary can mimic a separate gonadal component and karyotype with hormonal profile were valuable to settle the diagnosis. This highlights the importance of karyotyping and clinical presentation in differential diagnosis of ovotesticular disorders of sex development (OT-DSD), as imaging alone may struggle to differentiate between these structures without the presence of follicles or specific signal patterns.

Fig.8: Interobserver discordance in classic MRKH type 1 showing the triad. A 27 years old newly married lady complained of dyspareunia, giving history to 1ry amenorrhea. **A)** sagittal T2WI image demonstrate the midline triangular cord sign (yellow arrow). **B, C)** coronal T2WI images showed **M:** structures of intermediate T2 signal intensity (blue arrows) reported as ovotestes by observer 2 and as bilateral uterine buds by observer 1, both reported a relatively thick low signal fibrous band connecting between them (red arrow), which maintain caudal position relative to **O:** well- developed ovaries (white arrows) being closely related to their lower poles bilaterally. **V:** Axial and sagittal T2 images combined with complementary trans-perineal US (not shown here) revealed only canalization of the lower 2 cm of the vagina. No **E**xtrauterine anomalies. **D)** karyotyping reported 46 XX.

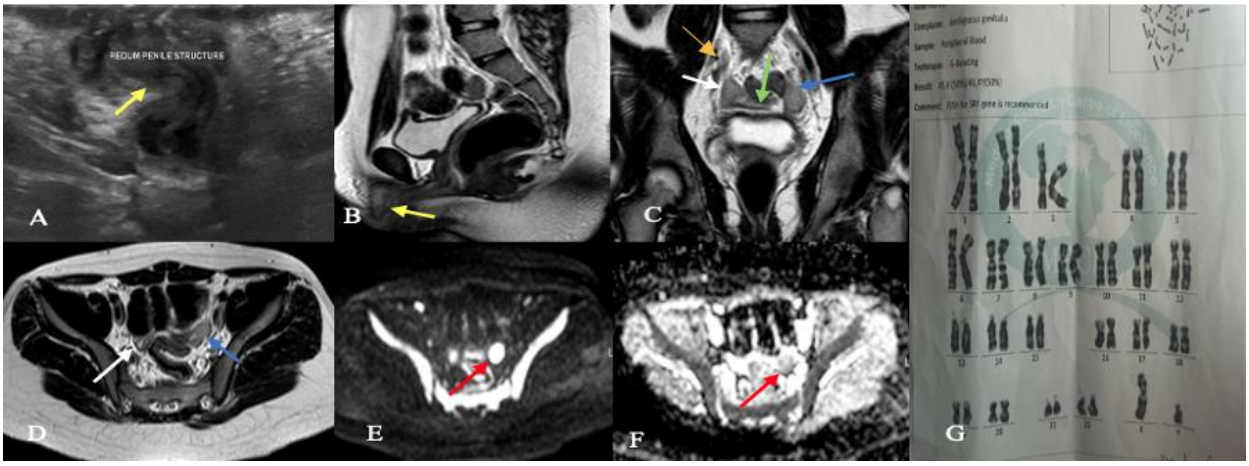
Cooper et al. noted that, although the timing of MRI within the menstrual cycle could theoretically affect the visibility of the endometrium, endometrial tissue should always be visible



once differentiation has occurred, and larger remnants had a significantly greater endometrial thickness, which makes them easier to identify [20]. Wang et al. [18] found that most remnants show single-layer differentiation, whereas 15.6% show two or three layers, hematometra, or hematosalpinx. Jaiswal et al. [2] stated that larger buds were associated with hematometra. In our study both observers identified zonal anatomy or thin endometrium in a subset of buds, which is clinically significant, because functional endometrium can cause cyclic pelvic pain or hematometra and may require surgery even in classic MRKH syndrome **(Fig. 9).**

Fig. 9: MRKH type 1 with functioning bud. A 16 years old girl referred for investigation of 1ry amenorrhea with right sided pelvic pain. **A, B) M**: coronal T2WI &T1WI revealed two uterine buds connected by thin converging band (red arrow) with the right one (blue arrow) is mildly distended by contents eliciting blood signal (high T1/ low T2). **O**: Both ovaries are of average size (thick orange arrows) **.C, D)** sagittal T2WIs showed midline triangular cord sign (yellow arrow) with canalization of distal 3 cm of the **V**agina. The distended uterine bud had no cervix (white arrow). No **E**xtrauterine anomalies.

The remaining patient with gonadal dysgenesis (1/12) had a different MRI pattern and presented with ambiguous genitalia. Pelvic MRI showed two homogeneous structures of intermediate T2 signal connected by a fibrous band, with diffusion restriction in the left one **(Fig. 10)**. The observers disagreed on the interpretation, and the senior radiologist resolved the case after



reviewing the karyotype, which revealed a 45,X/46,XY mosaic pattern (50%/50%). Surgical exploration confirmed that the left structure, initially suspected to be a uterine bud, was a dystrophic testis, whereas the contralateral structure was of Müllerian origin, and the diagnosis of mixed gonadal dysgenesis (MGD) was established. This case shows that a structure with diffusion restriction, in contrast to the intermediate signal and absent restriction of typical buds especially in presence of ambiguous genitalia, should raise suspicion of gonadal tissue, and that MRI findings need to be interpreted together with the karyotype and clinical data.

Fig.10: Mixed gonadal dysgenesis (MGD) :- 15 years old girl presented by 1ry amenorrhea. **A)** trans-perineal US revealed rudimentary penile structure that was also seen in sagittal T2 MRI series (yellow arrows).**B)** **M:** Absent midline triangular cord sign in T2 sagittal view**. C)** coronal T2WI revealed two homogenous intermediate signal structures with a low signal fibrous band connecting between them (green arrow) with **O:** streak ovarian tissue noted in the right side only (orange arrow). Non canalized **V**agina. **D)** axial T2WI showed the right (white arrows) and left (blue arrow) soft tissue structures with the right one showed central portion of high T2 (? Endometrial differentiation). **E, F)** DWI and ADC revealed diffusion restriction of the left structure. **G)** karyotyping reported 45XO (50%) and 46XY (50%). No **E**xtrauterine anomalies. The hormonal profile denoted menopausal levels of FSH 80.8 miU/ml and LH 32.2 miU/ml, while free testosterone was significantly high 10.3 pg/ml. The archived data reported surgical exploration and pathological confirmation of the right bud being Müllerian in origin (fibromuscular tissue), while the left one was dysgenetic testicular tissue.

Our case was consistent with the description of Giri et al. [21], who reported that MGD, arising from 45,X/46,XY mosaicism or rarer variants, is characterized by a dysgenetic testis on one side and a contralateral streak gonad, with a highly variable phenotype ranging from atypical genitalia to predominantly male or female presentations, and often with ipsilateral Müllerian remnants. MGD is a recognized cause of disorders of sex development, and early gonadectomy has traditionally been recommended to reduce the risk of gonadoblastoma

The midline triangular cord sign and the converging fibrous band are critical markers for identifying the caudal-most extent of Müllerian development. The fibrous band, present in 51.5% of the studied cases, serves as a bridge between lateralized uterine buds. This finding aligns with Boruah et al., who reported T2-hypointense converging bands in 77.8% of patients and the triangular cord sign in 44.4% [5]. In our study, the almost perfect interobserver agreement for these features ($\kappa = 0.88$ for the band and $\kappa = 0.91$ for the cord sign) reinforces MRI's reliability in detecting these subtle soft-tissue structures that might be missed on ultrasonography. In contrast, Bhayana et al. [14] reported poor to fair interobserver agreement for fibrous bands (κ: 0.2857 ± 0.3273 to 0.6032 ± 0.2149) and good for midline triangular soft tissue (κ: 0.7826 ± 0.1474). Most published literature indicated that the connecting fibrous band was identified in ~25–40% of MRKH patients [22].

Bud and ovarian volumes' assessment showed excellent interobserver agreement in our series. Schiau et al. [13] attributed the cranial position of the ovaries in MRKH to the absence of the fallopian tubes, and Haydardedeoglu et al. [23] described a rare unicornuate uterus with ipsilateral ovarian and renal agenesis. In gonadal dysgenesis, bud absence paralleled gonadal

absence, and in the unicornuate group, ipsilateral ovarian absence occurred in some patients without a rudimentary horn, as in the report of Zhang et al. [24].

Vaginal evaluation showed a shortened vagina with variable canalization in Müllerian agenesis, most often limited to the distal 2 cm. Interobserver agreement was almost perfect for vaginal canalization ($\kappa = 0.87$) and for vaginal length (Lin's CCC = 0.97). These findings agree with previous MRI series describing a short, blind-ending vaginal remnant that is often non-canalized or replaced by fibrous tissue [8,24]. Measuring the vaginal pouch and the degree of canalization is important for planning reconstruction, whether by dilator therapy or vaginoplasty [14].

Extrauterine anomalies evaluation showed almost perfect interobserver agreement ($\kappa = 0.96$), most often a renal anomaly (11/68, 16.2%). Schiau et al. [13] reported a higher prevalence of renal anomalies in MRKH, approaching 40%, with unilateral renal agenesis in about 15% of cases.

5. Conclusion:

The main diagnostic pitfall is a uterine bud that closely abuts or adheres to the ipsilateral ovary, which can be mistaken for a second gonadal component. In such cases, the MRI findings should be interpreted in conjunction with the karyotype, hormonal profile, and clinical examination before a final diagnosis is made. A structured MRI checklist allows reproducible assessment of Müllerian remnants and associated ovarian, vaginal, and extrauterine findings and may improve preoperative characterization and reduce uncertainty with suspected Müllerian developmental failure. The highest interobserver agreement was for the fibrous band, triangular cord sign, and for the volume and length measurements.

Limitations:

The main limitation is the lack of histopathological confirmation of the Müllerian remnants, since surgery solely for diagnosis was not clinically indicated. The study therefore assessed interobserver agreement rather than diagnostic accuracy against a histological reference standard. In addition, the retrospective, single-center design and the small sample size, particularly in the less frequent diagnostic subgroups, may limit generalizability. The final diagnosis integrated imaging, clinical data, and karyotype when available, so the contribution of each component could not be evaluated separately. Another pitfall was that uterine buds are small structures, and measurements and detection on T2-weighted images with a slice thickness of 5 mm may be affected by partial-volume averaging, particularly where a bud abuts the ovary, and this may have contributed to the disagreement between observers, including the interpretation of five bud-like structures as the second gonadal component of an ovotestis by one observer. Finally, the MOVE checklist should be validated in larger, prospective, multicenter studies.

Recommendation:

Future studies should use thin-slice or 3D isotropic T2-weighted sequences for scanning Müllerian remnants, with diffusion-weighted imaging and ADC measurements, to improve the delineation of small remnants and their separation from adjacent gonadal tissue.

6. List of Abbreviations:

MRI Magnetic resonance imaging

CCC Concordance correlation coefficient

MRKH Mayer–Rokitansky–Küster–Hauser Syndrome

ASRM American Society for Reproductive Medicine

AFS American Fertility Society

US Ultrasound

CAIS Complete Androgen insensitivity Syndrome

PACS Picture Archiving and Communication System

TVUS Transvaginal ultrasound

T1WI T1-weighted image

T2WI T2-weighted image

DWI Diffusion-weighted image

SD Standard deviation

IQR Interquartile range

ROI Region of interest

HSG Hysterosalpingography

DSD Disorders of sex development

MGD Mixed gonadal dysgenesis

7. References

1. Dixit R, Duggireddy CS, Pradhan GS (2025) Mullerian anomalies: revisiting imaging and classification. Insights Imaging 16:40.
2. Jaiswal S, Prasad U, Gupta R, Kumari M (2023) Magnetic resonance imaging in patients of Mayer-Rokitansky-Kuster-Hauser (MRKH) syndrome presenting with primary amenorrhoea: a prospective study. Egypt J Radiol Nucl Med 54(1):69.
3. Pfeifer SM, Attaran M, Goldstein J, Lindheim SR, Petrozza JC, Rackow BW et al (2021) ASRM Müllerian anomalies classification 2021. Fertil Steril 116(5):1238–1252.
4. Alqarni A, Alqahtani NS, Al-Shehri M, Abdelhady HA, Alqahtani NS Jr (2025) Unicornuate uterus with a non-communicating rudimentary uterine horn treated via laparoscopic resection

with preservation of both ovaries and fallopian tubes: a case report and review of the literature. Cureus 17(2).

5. Boruah DK, Sanyal S, Gogoi BB, Mahanta K, Prakash A, Augustine A et al (2017) Spectrum of MRI appearance of Mayer-Rokitansky-Kuster-Hauser (MRKH) syndrome in primary amenorrhea patients. J Clin Diagn Res 11(7):30.
6. Sugi MD, Penna R, Jha P, Poder L, Behr SC, Courtier J et al (2021) Müllerian duct anomalies: role in fertility and pregnancy. Radiographics 41(6):1857–1875.
7. Fraccascia B, Sodero G, Pane LC, Malavolta E, Gola C, Pane L et al (2024) Complete androgen insensitivity syndrome in a young girl with primary amenorrhea and suspected delayed puberty: a case-based review of clinical management, surgical follow-up, and oncological risk. Diseases 12(10):235.
8. Yoo RE, Cho JY, Kim SY, Kim SH (2013) Magnetic resonance evaluation of Müllerian remnants in Mayer-Rokitansky-Küster-Hauser syndrome. Korean J Radiol 14(2):233–239.
9. Nakamata A, Matsuki M, Otake Y, Himoto Y, Kaneko Y, Nakaya M et al (2024) Magnetic resonance imaging features of complete androgen insensitivity syndrome in comparison to Mayer-Rokitansky-Küster-Hauser syndrome. Abdom Radiol (NY) 49(9):3220–3231.
10. Cohen J. A coefficient of agreement for nominal scales. Educational and psychological measurement. 1960 Apr;20(1):37-46.
11. Landis JR, Koch GG. The measurement of observer agreement for categorical data. biometrics. 1977 Mar 1:159-74.
12. Lin LI. A concordance correlation coefficient to evaluate reproducibility. Biometrics. 1989;45(1):255–268.

13. Schiau C, Csutak C, Ciurea AI, Pintican R, Dulgheriu IT, Manole S (2026) Mayer-Rokitansky-Kuster-Hauser syndrome: from radiological diagnosis to further challenges—review and update. Diagnostics (Basel) 16(1):138.
14. Bhayana A, Ghasi RG (2019) MRI evaluation of pelvis in Mayer-Rokitansky-Kuster-Hauser syndrome: interobserver agreement for surgically relevant structures. Br J Radiol 92(1097):20190045.
15. Yang EC, Elbasueny B, Bacal V, Bedaiwy MA (2022) American Society for Reproductive Medicine (ASRM) Mullerian anomalies classification 2021 (MAC 2021): prevalence in a recurrent pregnancy loss (RPL) population. Fertil Steril 118(4):E180.
16. Chen N, Song S, Bao X, Zhu L (2022) Update on Mayer-Rokitansky-Küster-Hauser syndrome. Front Med 16(6):859–872.
17. Herlin MK, Petersen MB, Brannstrom M (2020) Mayer-Rokitansky-Küster-Hauser (MRKH) syndrome: a comprehensive update. Orphanet J Rare Dis 15(1):214.
18. Wang Y, He YL, Yuan L, Yu JC, Xue HD, Jin ZY. Typical and atypical pelvic MRI characteristics of Mayer-Rokitansky-Küster-Hauser syndrome: a comprehensive analysis of 201 patients. Eur Radiol. 2020;30:4014–22.
19. Jha SK, Manandhar R, Shrivastava VR (2019) Coexistence of gonadal dysgenesis and Mullerian agenesis in a female with 46,XX karyotype: a case report. JNMA J Nepal Med Assoc 57(216):119.
20. Cooper N, Al-Memar M, Linton-Reid K, Edmonds K, Rose G, Dixon N, McNamara C, Fotopoulou C, Ree KV, Bharwani N. Magnetic resonance imaging and clinical features of Mayer–Rokitansky–Küster–Hauser syndrome: A 10-year review from a dedicated specialist centre. BJOG: An International Journal of Obstetrics & Gynaecology. 2025 Jan;132(1):64-71.

21. Giri D, Yewale S, Hickingbotham H, Williams C, Shalaby M, Alderson J et al (2026) Mixed gonadal dysgenesis: a comprehensive review of clinical spectrum, diagnostic strategies, and management approaches. Clin Endocrinol (Oxf) 104(2):92–102.
22. Hall-Craggs MA, Williams CE, Pattison SH, Kirkham AP, Creighton SM (2013) Mayer-Rokitansky-Kuster-Hauser syndrome: diagnosis with MR imaging. Radiology 269(3):787–792.
23. Haydardedeoglu B, Simsek E, Kilicdag EB, Tarim E, Aslan E, Bagis T (2006) A case of unicornuate uterus with ipsilateral ovarian and renal agenesis. Fertil Steril 85(3):750.e1-750.e3.
24. Zhang H, Zhang Y, Bao L, Ning G (2023) MRI presentations of Müllerian duct anomalies in association with unilateral renal agenesis. Clin Radiol 78(3):168–174.

Supplementary Files

This is a list of supplementary files associated with this preprint. Click to download.

- MOVEchecklist.pdf